5-3 Optical Communication Experiments at DLR

Dirk Giggenbach, Florian Moll, and Nicolas Perlot

In 2006 and 2009, the Institute of Communications and Navigation (IKN) of the German Aerospace Center (DLR) in a joined venture together with JAXA and NICT executed optical downlink experiments with JAXA's OICETS/Kirari to investigate the optical LEO downlink channel and evaluate the feasibility of this transmission technology for future applications. The DLR Optical Ground Station at Oberpfaffenhofen near Munich comprised several devices for measuring the effect of the atmosphere's index-of-refraction turbulence (IRT) and a data receiver frontend to quantify bit-error distributions. This project was named KIODO (KIrari Optical Downlinks to Oberpfaffenhofen). Results showed a strong dependency on link elevation for all IRT-related parameters. These two successful measurement campaigns encouraged DLR-IKN to develop a laser test source for various small LEO missions to enable further investigations and optimizations of this technology for future telemetry data down- and up-links.

Keywords
Free-space optical communication, Atmospheric propagation, Laser beam transmission, Scintillation index

1 Introduction

The optical communications group (OCG) of DLR-IKN has been working on optical free-space data links for atmospheric and space applications for more than fifteen years, resulting in several experimental laser transceiver terminals and the building of the Optical Ground Station Oberpfaffenhofen (OGS-OP). Encouraged by contacts with NICT, in summer 2005 negotiations between DLR and JAXA were initiated to use OGS-OP for reception of the laser signal from JAXA's laser terminal LUCE onboard OICETS/Kirari. This resulted in the first optical LEO downlinks to European grounds in June 2006, after JAXA and NICT had performed first successful downlinks to NICT's OGS at Koganei within the KODEN experiment [1]. In summer 2009 a second downlink campaign was initiated by NICT under the umbrella of GOLCE [2], together with further ground stations of JPL, ESA and again, NICT.

For the first campaign in summer 2006 the telescope of OGS-OP was sheltered in a fully opening clam-shell dome to allow tracking of objects with fast azimuth velocity. The telescope's focus optics was fitted with several beam-splitters to illuminate different index-of-refraction turbulence (IRT) measurement devices like DIMM (differential image motion monitor, to measure the Fried-parameter), a pupil camera (for measurements of the intensity distribution in the pupil plane), the tracking camera, a power meter, and the data receiver frontend. Furthermore, a separate 5 cm refractor telescope was also used for power measurements, which is useful to compare aperture averaging influence of small to large receiver apertures. For the second campaign, in 2009, a focal spot camera, a high speed data logger for the received analog data signal, and a Shack-Hartmann wavefront sensor (SHWFS) were added. An overview of measurement instruments applied in the corresponding campaign is given with Table 1.

Table 1 *List of applied measurement instruments. All instruments are attached to the optical bench of the 40 cm Cassegrain telescope except for a separate 5 cm aperture power meter co-aligned to the telescope*

Measurement	Campaign
Power meter (40 cm)	2006/2009
BERT	2006/2009
DIMM	2006/2009
Focus camera	2009
SHWFS	2009
Pupil camera	2006/2009
Data logger	2009
Power meter 5 cm	2006/2009

The power meter consists of a standard silicon receiver on the telescope's optical bench. The bit-error rate tester (BERT) determines bit-error rate of the received PRBS data signal. The DIMM is meanwhile a standard instrument in astronomy to measure the Fried parameter r_0. The pupil camera and the focus camera record images of the pupil plane intensity distribution and focal intensity pattern, respectively, and the SHWFS can capture information about the phase and intensity of the complex optical field.

Acquisition of Kirari's signal was initiated by open-loop pointing of two laser beacons with divergence larger than the orbital position uncertainty of the satellite. When LUCE detected this signal from ground, it sent its own laser beam towards OGS-OP, which was detected by a co-aligned wide field-of-view camera (WFoV). After correcting the telescope's pointing direction with this first signal, OGS-OP switched to its narrow field-of-view (NFoV) camera, which tracked LUCE's signal with a precision below 50 μrad during the satellite pass. This tracking precision allowed illumination of all measurement devices and the receiver frontend during the whole experiment. The most important characteristica of OGS-OP is listed in table 2.

Table 2 *Parameters of OGS-OP telescope and tracking. WFOV and NFOV denote the field of view of the respective tracking camera*

Telescope type	Cassegrain
Telescope focal length	3.6 m
Aperture diameter	40 cm
Central obscuration	12 cm
WFoV Tracking FoV	165 × 123 mrad
WFoV Tracking focal length	50 mm
NFoV tracking FoV	3.5 × 2.6 mrad
NFoV tracking focal length	2.0 m
RFE FoV	0.7 mrad
RFE Focal length	1.4
Beacon divergence (each)	5 mrad ($1e^{-2}$)

2 KIODO 2006 - downlink experiments in 2006

Table 3 provides an overview of the 8 trials that have been done during the KIODO 2006 experiment campaign. A trial corresponds to a single particular pass of the OICETS satellite, i.e. one particular experiment. More frequent links were not possible because, for each trial, OICETS requires a special attitude configuration that must be planned some days in advance [3].

All trials took place in the night at approximately the same local time. Viewed from the ground station, satellite passes have different maximum elevation angles. The operation of the optical terminal LUCE onboard OICETS had some constraints regarding its angular speed and the position of the Sun with respect to its field of view. Due to these constraints, each trial was limited to a predetermined pass segment and a corresponding elevation span (5th column in Table 3). Because of cloud coverage, no link was established in trials 5, 6 and 8 of the 2006 campaign.

OICETS is optically compatible with the terminal onboard ESA's ARTEMIS satellite and therefore transmits data at 50 Mbit/s with an OOK modulation and at a wavelength of 847 nm and receives optical signals with wavelengths near 810 nm. The KIODO downlink involves two beams: the beacon beam

Table 3 *Overview of the KIODO trials. Local time is UTC + 2 hours*

KIODO Trial	Day of June 2006	Time (UTC) of Pass Start	Maximum Pass Elevation	Measurement Elevation Span	Weather	Remark
KT06-1	7th	1:13	45.5°	10–35°	90% clear sky, 8°C	No scintillation / DIMM measurement
KT06-2	9th	0:02	33.5°	10–32°	90% clear sky, 10°C	No BER measurement
KT06-3	14th	1:04	55.6°	10–45°	clear sky, 10°C	
KT06-4	15th	23:54	28.0°	2–27°	80% clear sky, 12°C	
KT06-5	21st	0:56	68.2°		Cloudy	No Link
KT06-6	23rd	1:21	38.4°		Cloudy	No Link
KT06-7	28th	0:47	83.2°	4–43°	Thunder clouds 1 h before trial, 18°C	
KT06-8	30th	1:12	46.5°		Cloudy	No Link

from the ground station (wavelength of 808 nm, divergence of 5 mrad) and the communication beam from OICETS (divergence of 5 µrad [4]).

In 2006 the OGS-OP consisted of a 40-cm Cassegrain telescope supported by an astronomical mount. The telescope and the mount can be seen in Fig. 1. The communication receiver, the tracking camera, the measurement cameras and a power-meter are located on a metal plate fixed behind the telescope. The beacon beam was transmitted by two spatially displaced 5-cm telescopes mounted on each side of the 40-cm telescope.

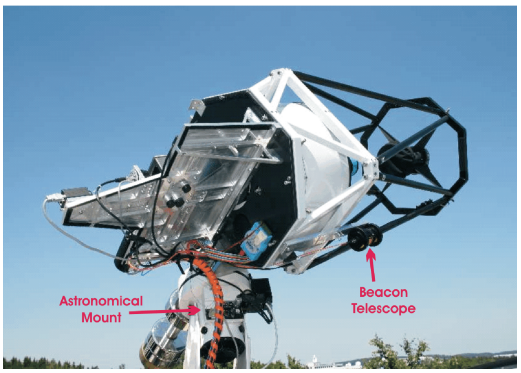

Fig.1 *View of the focal bench of the 40-cm telescope of OGS-OP in June 2006, then still with a conventional astronomical mount*

3 KIODO 2009-downlink experiments in 2009

The second KIODO experiment campaign took place between 24th June and 4th September 2009. Table 4 provides an overview of the trials that have been done during that KIODO campaign. In total, ten trials were conducted, whereas only five trials have been successful due to bad weather conditions. In trial number seven, link acquisition could be obtained despite a partly cloudy sky. However, the link was blocked after a short time and therefore, the measurements are not useful. In the experiments 1, 2, 4, 9 and 10, cloud occurrence prohibited even link acquisition.

In 2009, the OGS-OP telescope was hosted by a somewhat different mount system than in 2006. A custom-made fork mount construction with high-performance precision rotation stages was applied. This mount and the motors can bear a quite heavy load and is flexible to have little restrictions on the installation of experiment devices. In Figure 2, the new mount in the clamshell dome is shown (left). The measurement setup in the optical bench behind the telescope is illustrated on the right side. In comparison to the experiments in 2006, the fo-

Table 4 *Overview of the KIODO trials in 2009. Local time is UTC + 2 hours*

KIODO Trial	Date 2009	Time (UTC) of Pass Start	Maximum Pass Elevation	Measurement Elevation Span	Weather	Remark
KT09-01	24th Jun	02:01	64.0°	-	Rain	No Link
KT09-02	26th Jun	00:44	21.0°	-	Rain	No Link
KT09-03	1st Jul	01:28	57.2°	11–57°	Almost clear sky	
KT09-04	3rd Jul	01:46	86.8	-	Overcast	No Link
KT09-05	19th Aug	02:20	45.7°	3–35°	Almost clear sky	
KT09-06	21st Aug	01:03	27.2°	10–27°	Clear sky	
KT09-07	26th Aug	01:47	78.3°	6–7°	Cloudy, drizzle	
KT09-08	28th Aug	02:04	68.8°	4–49°	Clear sky	
KT09-09	2nd Sep	01:13	33.4°	-	Overcast	No Link, one flash spotted
KT09-10	4th Sep	01:31	51.1°	-	Overcast, rain	No Link

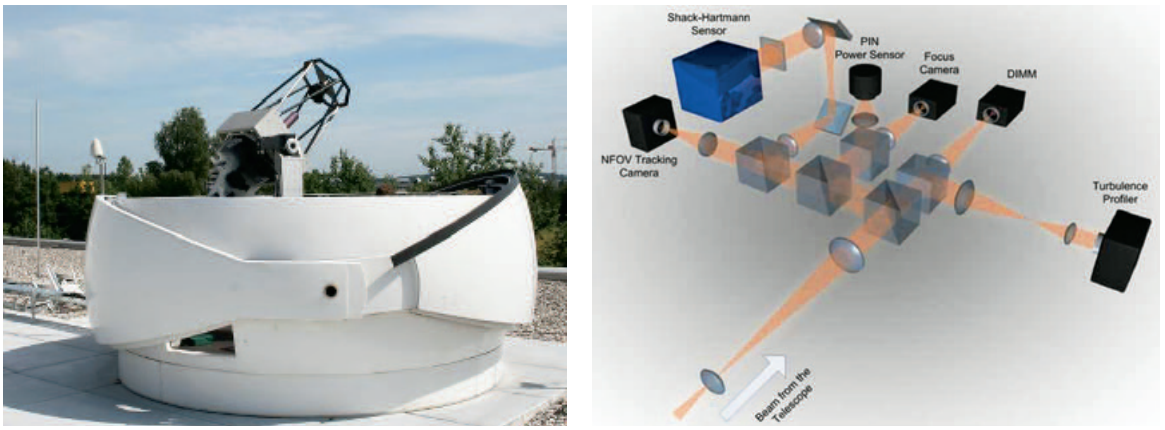

Fig.2 *Image of receiver telescope in June 2009, hosted by an astronomical clamshell dome (left) and Instrument setup in the 2009 campaign (right). The beam is guided to the tracking camera, receiver front-end and measurement instruments* [5]

cus camera and Shack-Hartmann sensor are added.

4 Measurement results and scientific findings

To some extent, analysis of both KIODO measurement campaigns has been performed and the results published [4] [6]-[8]. A representative example of recorded power with the 40 cm aperture is given in Fig. 3 (left). With elevation, mean power is increasing and the fluctuations are clearly visible. The power drop down from around 24° was caused by a thin cloud. In the same figure on the right, this power vector is plotted normalized to the instantaneous mean. Here, it is very illustrative that relative power fluctuation decreases significantly with rising satellite elevation angle.

In Figure 4, the downlink power scintillation index for seven satellite passes in 2006 and 2009 is shown. The power records of both campaigns are used to determine scintillation behavior for different atmospheric conditions and indicate its variability for our particular location. As expected, the power fluctuation index decreases significantly with higher ele-

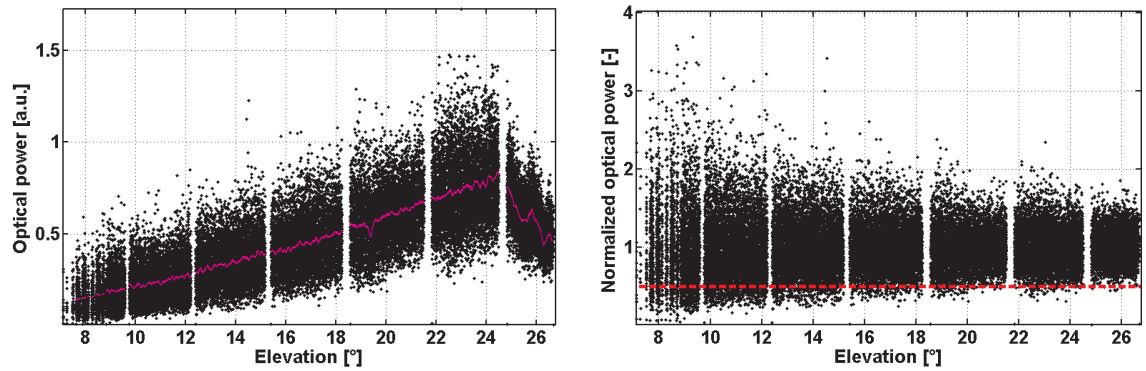

Fig.3 *Left: Received power at KT06-04 in arbitrary units. The black values are the power samples recorded at 10 kHz. The magenta line is the 1 s sliding window mean. Right: Normalized received power. The black values are the normalized power samples recorded at 10 kHz rate. The dashed red line marks the –3 dB fading-threshold with respect to unity mean* [8]

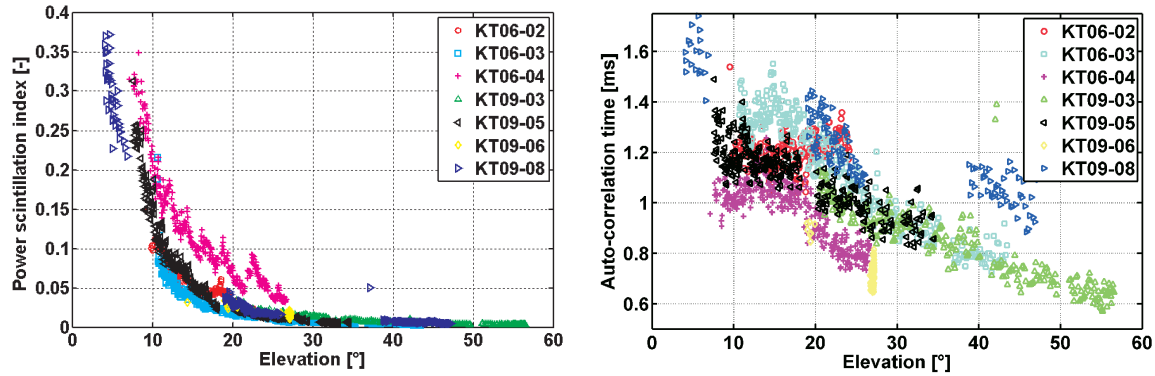

Fig.4 *Power scintillation index for all KIODO measurements with the 40 cm aperture (left) and auto-correlation time as defined by the 50% roll-off of the auto-correlation function (right)* [8]

vations, but the effect of saturation is not visible at low elevations due to the aperture averaging effect. In contrast, in intensity scintillation we do observe the saturation effect below 10- elevation, resulting in a peak of the curve (compare Fig. 5 left). The correlation time for reception with 40 cm aperture is also shown in Fig. 4 (right). Here, the run of the curves shows a local maximum for particular experiments, e.g. KT06-03 and KT06-04.

The scintillation correlation time is essentially determined by the ratio of the scintillation correlation width to the transversal beam speed relative to the turbulence cells (i.e. relative to the air). Below a certain elevation angle, the correlation width starts decreasing as a result of scintillation saturation [6][9]. The transversal beam speed increases with elevation because the satellite's transversal speed increases. As a result of these effects, a global maximum was observed at about 13° elevation which is approximately the limit between the saturation regime and the weak-fluctuation regime.

As a consequence of Taylor's frozen-turbulence hypothesis, the correlation time decreases as the receive aperture size increases. However, the global maximum is expected to remain approximately at the same elevation.

In Figure 5, values of the scintillation index and the Fried parameter are given for passes in 2006. On a first camera, pupil images

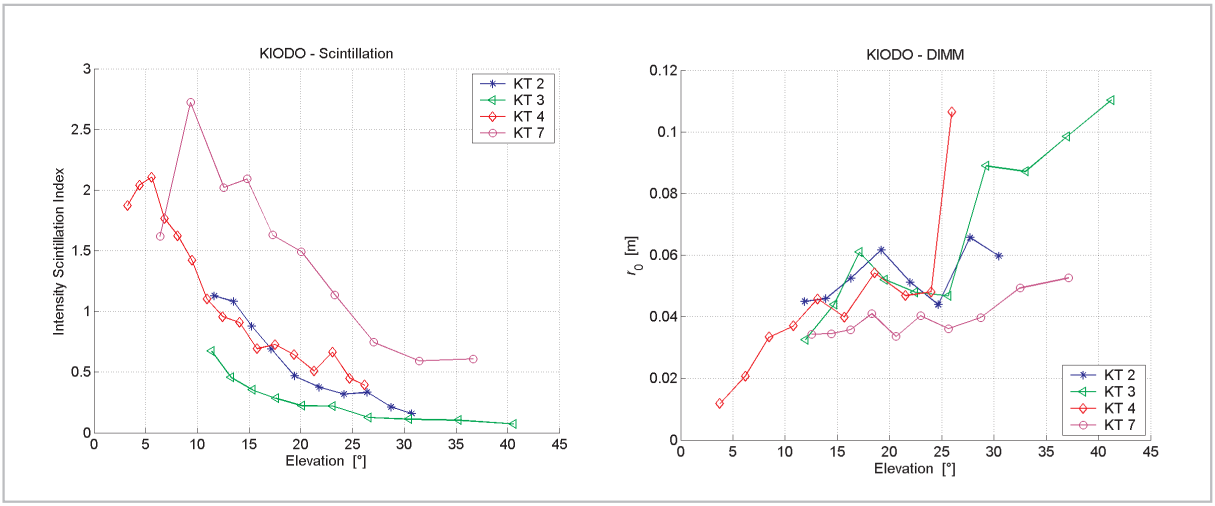

Fig.5 *Intensity scintillation index of the downlink and r_0 measurements from the DIMM instrument* [4]

have been recorded to measure scintillation. With a second camera, the Fried parameter r_0 was estimated using the DIMM concept [10]. Both cameras had an exposure time of 80 µs which is short enough to "freeze" the images in time.

The scintillation index for a point receiver (i.e., values of camera pixels were considered) using the 40-cm diameter aperture is shown in Fig. 5, left, as a function of elevation. The scintillation dynamic was fully rendered by the 12-bit resolution of the pupil camera. The two different apertures allow the assessment of the spatial averaging of scintillation over the aperture. Over the aperture of 40-cm diameter (secondary-mirror obscuration of 12-cm diameter), the aperture averaging factor was approximately 0.2 and 0.1 at 5° and 30° elevation, respectively.

As predicted by theory [9], we observed saturation of scintillation for a point receiver at low elevations. Also interesting is the large variation of the scintillation between two different nights: scintillation during KT06-07 was 5 times stronger than during KT06-03. The main difference between the two trials is the presence of a warm thunderstorm a few hours before KT06-07.

Curves of Fig. 5 can be compared to the theoretical values of Table 5. Theoretical values at 30° elevation are within the range of the measured data. Although the $HV_{5\text{-}7}$ atmospheric turbulence profile is considered a day-time model, its applicability to the nighttime atmosphere of Oberpfaffenhofen can be considered. The variability of the channel parameters that were all measured in the middle of the night is quite unexpected and means that the design of an optical communication system shall be based on a worst turbulence case.

Table 5 *Theoretical values of the intensity scintillation index σ_I^2 and Fried parameter r_0 as given by the Rytov theory together with the $HV_{5\text{-}7}$ turbulence model*

	30° elevation	90° elevation
σ_I^2	0.45	0.13
r_0 [m]	0.062	0.093

5 Considerations for applying adaptive optics

The full information about the received beam can be obtained applying a wave-front sensor that measures the optical field in intensity and phase. In 2009, a Shack-Hartmann type of these sensors was setup on the optical bench, running at a frame rate of around 1 kHz. The most essential information which can be obtained from these measurements is the phase of the incident beam, i.e. its wave-front distortions. The phase probability density function for the experiment KT09-08 for sev-

eral elevation angles is depicted in Fig 6. With lower elevations, the Gaussian-shaped function broadens which proves the higher degree of distortion for lower viewing angles. Note that a standard algorithm for wave-front reconstruction was used in this analysis and therefore, phase values for elevations below 20° might be underestimated [5]. For elevation angles above 20°, the measurements are valuable to predict phase aberrations in the receiver plane and develop design rules for adaptive optics (AO) systems.

The central element of such an AO system would be the actuator, in most cases a deformable mirror, which ideally forms an inversion of the wave-front to remove the distortions. Its peak-to-peak aberration is about five times the standard deviation. Because the mirror moves only half the distance of the distortion, a general rule of thumb for the actuator stroke is to be 2.5 times the wave-front standard deviation [11]. Combining this rule with the model estimation of tilt-corrected standard deviation in [12] results in

$$Stroke = {}^{5}\!/_{2} \cdot 0.366 \cdot \left({}^{D}\!/_{r_0}\right)^{5/6} \quad \text{[rad]} \qquad (1)$$

where D is the receiver aperture and r_0 the Fried diameter. Thus, the necessary stroke increases with aperture size and decreasing Fried parameter. Figure 6 shows a wave-front standard deviation of 1.2 rad around 20° leading to a mirror stroke of 3.0 rad. With a wavelength of 847 nm, the actual necessary stroke length would be 0.4 µm. For Fried parameter as low as 1 cm, which may occur at elevations well below 5°, Equation (1) predicts a mirror stroke of 19.8 rad (or 2.7 µm). Eventually, these strokes are easily obtainable with off-the-shelf components. However, time behaviour of phase distortions is not considered here and is another important, rather challenging aspect for choice of the proper components.

Estimating the Fried parameter r_0 with standard methods based on long-term wave-front observations is not adequately applicable for a LEO downlink: The Fried parameter is by definition a long-term parameter whereas the volume traversed by the optical signal is changing rapidly during a downlink with the slew of the line of sight. Instead, one has to acquire fast time series of a suitable parameter, and calculate averages for different observation time windows. This was done with a method based on the short-term tilt-removed focal seeing disk diameter, for KT09-08, as

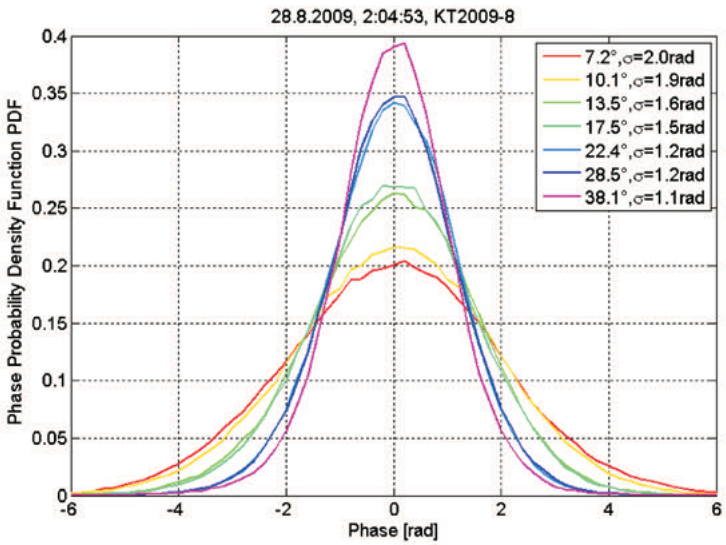

Fig.6 *Unwrapped phase Probability Density Function (PDF) recorded by the Shack-Hartmann sensor during the SGLs from OICETS 2009, trial 8. Several elevation angles are shown. Averaging time for the evaluation was 10.7 s (100 frames)* [5]

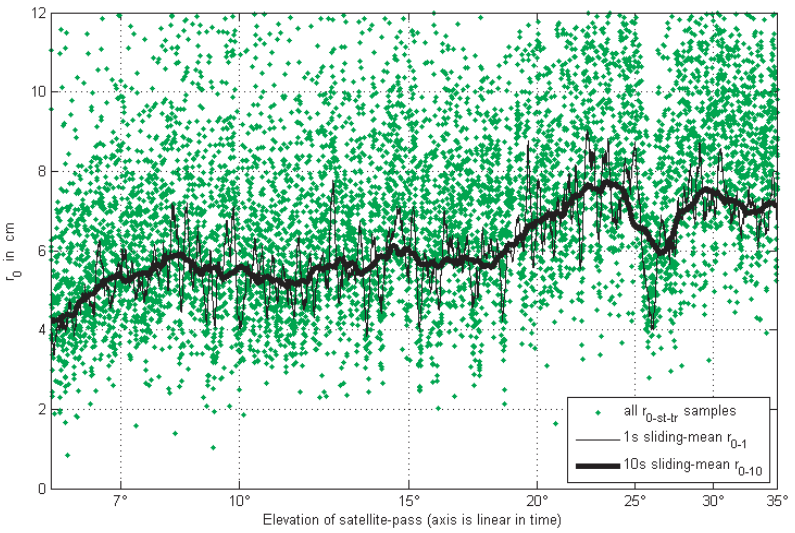

Fig.7 *Comparison of different averaging times (short-term, 1 s and 10 s) for r_0 estimation in the optical satellite downlink for KT09-08. The increase of r_{0-10} (averaging time of 10 seconds) with elevation during the satellite's ascending path over the OGS-OP coincides with theory (less air mass in the link path at higher elevations), the unsteady behaviour of this curve is caused by intermittent turbulent layers traversed by the link. Green dots are the short-term values, which show a significant variance*

described in [13]. These can be further translated into instantaneous values for r_0 and its longer-term averages, as shown in Fig. 7. This investigation helps in analyzing the resolution requirements for an adaptive optic system, and allows estimation of a coherent, or fiber-coupled, receiver's performance based on short-term heterodyne-efficiency statistics.

6 Summary and outlook

KIODO experiments to DLR's OGS provided extremely valuable information on the optical LEO downlink transmission channel:

- Scintillation saturation as predicted by theory could be observed at low elevations (< 10°).
- The beneficial effect of aperture averaging on scintillation was clearly observed and downlink terminal aperture sizes can be optimized accordingly in future operational systems.
- A mild increase of the scintillation speed with the elevation as a result of a faster link slew rate was observed.
- Measurements of wave-front distortions allow the performance evaluation of future single-mode receivers (i.e., coherent or fiber-coupling receivers). The necessity of applying adaptive optics technology can be considered and specifications of such systems set.
- The feasibility of link acquisition at very low elevations (< 3°) with multiple beacons was demonstrated.
- Prediction of channel behavior dependent on satellite pass geometry is possible when combining with local weather and topological constraints. However, a much broader database is required for reliable predictions.
- Adaption of system parameters like data-rate, code-rate, modulation scheme, inter-leaver size to instantaneous channel state can be considered [14].

Ongoing work at DLR-IKN-OCG includes the installation of a new Optical Ground Station Oberpfaffenhofen (OGS-OP), which was necessary after relocation of the institute to a new building (see Fig. 8). To enable performance of downlinks to miscellaneous experimental ground station locations on Earth, the

Transportable Optical Ground Station (TOGS) was developed and is currently put into operation (Fig. 9). Future optical downlink experiments include tests with OSIRIS, DLR's own laser source in space.

Future laser transmission activities shall be pursued including daytime measurements, transmission at other wavelengths, and testing of suitable channel coding to compensate the strong fading.

The authors want to thank JAXA and NICT for supporting the KIODO experiments and for the excellent cooperation. Further we are grateful to the members of DLR-IKN-OCG for their commitment to perform the downlinks during all times of day and mostly in the middle of the night.

Fig.8 *The dome of the new OGS-OP on top of the building of DLR's Institute for Communications and Navigation*

Fig.9 *Transportable Optical Ground Station of DLR for Satellite- and Aircraft-Downlinks, with transport vehicle*

References

1 M. Toyoshima, K. Takizawa, T. Kuri, W. Klaus, M. Toyoda, H. Kunimori, T. Jono, Y. Takayama, N. Kura, K. Ohinata, K. Arai, and K. Shiratama, "Ground-to-OICETS laser communication experiments," Proc. of SPIE, 6304B, 1–8, 2006.

2 Proceedings of International Workshop on Ground-to-OICETS Laser Communications Experiments 2010 (GOLCE 2010), ISSN 2185-1484, Tenerife, Spain, May 2010.

3 Y. Takayama, T. Jono, M. Toyoshima, H. Kunimori, D. Giggenbach, N. Perlot, M. Knapek, K. Shiratama, J. Abe, and K. Arai, Tracking and pointing characteristics of OICETS optical terminal in communication demonstrations with ground stations, Free-Space Laser Communication Technologies XIX, Proc. of SPIE, 6457A, 2007.

4 T. Jono, Y. Takayama, N. Perlot, et al., "Report on DLR-JAXA Joint Experiment: The Kirari Optical Downlink to Oberpfaffenhofen (KIODO)," JAXA, ISSN 1349-1121, 2007.

5 M. Knapek, "Adaptive Optics for the Mitigation of Atmospheric Effects in Laser Satellite-To-Ground Communications," Ph.D. dissertation, Technische Universität München, Munich, Germany, 2011.

6 N. Perlot, M. Knapek, D. Giggenbach, J. Horwath, M. Brechtelsbauer, Y. Takayama, and T. Jono, "Results of the Optical Downlink Experiment KIODO from OICETS Satellite to Optical Ground Station Oberpfaffenhofen (OGS-OP)," Proc. of SPIE Vol. 6457, 2007.
7 F. Moll, "KIODO 2009: Trials and analysis," International Workshop on Ground-to-OICETS Laser Communications Experiments 2010: GOLCE 2010, 2010, pp. 161–171.
8 F. Moll and M. Knapek, "Free-space laser communications for satellite downlinks: Measurements of the atmospheric channel," in Proceedings of the 62nd International Astronautical Congress, 2011.
9 L. C. Andrews and R. L. Phillips, Laser Beam Propagation through Random Media, SPIE Press, Bellingham, Washington, 2005, 2nd edition.
10 M. Sarazin and F. Roddier, "The ESO differential image motion monitor," in Astronomy and Astrophysics, Vol. 227, Issue 1, pp. 294–300, 1990.
11 R. K. Tyson, Introduction to Adaptive Optics. SPIE Press, Bellingham, 2000.
12 R. Noll, "Zernike polynomials and atmospheric turbulence," in Journal of the Optical Society of America A: Optics, Image Science, and Vision, Vol. 66, Issue 6, 1976, pp. 207–211.
13 D. Giggenbach, "Deriving an estimate for the Fried parameter in mobile optical transmission scenarios," Applied Optics, Vol. 50, No. 2, 10 Jan. 2011.
14 D. Giggenbach et al., "Space Communications Protocols for Future Optical Satellite-Downlinks," 62nd International Astronautical Congress, Cape Town, South Africa, 2011.

(Accepted March 14, 2012)

***Dirk Giggenbach**, Dr. Eng.*
German Aerospace Center, Team Leader Advanced Optical Technologies
Atmospheric Optical Communications
dirk.giggenbach@dlr.de

Florian Moll
Aerospace Center, Group member Optical Communication Systems
Atmospheric Optical Communications
florian.moll@dlr.de

Nicolas Perlot
Aerospace Center, Group member Advanced Optical Technologies
Atmospheric Optical Communications
nicolas.perlot@dlr.de